

Identification of Signal, Noise, and Indistinguishable Subsets in High-Dimensional Data Analysis

X. Jessie Jeng

Abstract

Motivated by applications in high-dimensional data analysis where strong signals often stand out easily and weak ones may be indistinguishable from the noise, we develop a statistical framework to provide a novel categorization of the data into the signal, noise, and indistinguishable subsets. The three-subset categorization is especially relevant under high-dimensionality as a large proportion of signals can be obscured by the large amount of noise. Understanding the three-subset phenomenon is important for the researchers in real applications to design efficient follow-up studies. We develop an efficient data-driven procedure to identify the three subsets. Theoretical study shows that, under certain conditions, only signals are included in the identified signal subset while the remaining signals are included in the identified indistinguishable subsets with high probability. Moreover, the proposed procedure adapts to the unknown signal intensity, so that the identified indistinguishable subset shrinks with the true indistinguishable subset when signals become stronger. The procedure is examined and compared with methods based on FDR control using Monte Carlo simulation. Further, it is applied successfully in a real-data application to identify genomic variants having different signal intensity.

Keywords: Two-Level Thresholding; Signal detection; False positive control; False negative control; Multiple testing; Variable screening.

X. Jessie Jeng is an Assistant Professor in the Department of Statistics, North Carolina State University, 27695.

1 Introduction

The problem of identifying a small number of signals from a large amount of noise is a central topic in modern statistics due to motivations from a wide spectrum of emerging applications. Examples include the detection of astrophysical sources, surveillance for disease outbreaks, identification of causal genetic markers, etc. In real applications, it is frequently observed that strong signals can easily stand out, while weak ones are often mixed indistinguishably with the noise. This phenomenon is especially relevant under high-dimensionality as a large proportion of signals can be obscured by the large amount of noise..

In this paper, we aim to extract valuable information from the data by categorizing the data into the signal, noise, and indistinguishable subsets. More specifically, we want to identify the signal subset in the data which includes only true signals, the noise subset which includes only noise, and the indistinguishable subset, where signals and noise cannot be separated. To formulate the problem rigorously, let S_0 be the collection of noise in the data, and S_1 the collection of true signals. The p-value of the data

$$P_i \sim U1_{\{i \in S_0\}} + G1_{\{i \in S_1\}}, \quad i \in \{1, \dots, n\}, \quad (1)$$

where U is the uniform distribution on $[0, 1]$ and G is some unknown continuous distribution with $G(t) > U(t)$ for all $t \in (0, 1)$. The p -values are ordered as $P_{(1)} \leq P_{(2)} \leq \dots \leq P_{(n)}$. Define d_* as the separation point between the signal and indistinguishable subsets, and d_{**} the separation point between the indistinguishable and noise subsets, i.e. $d_* = \min\{i : P_{(i)} \text{ from a noise}\} - 1$ and $d_{**} = \max\{i : P_{(i)} \text{ from a signal}\}$. Our goal is to identify the three subsets by estimating d_* and d_{**} .

Understanding the three-subset phenomenon can be important for the researchers in real applications to design appropriate follow-up studies and allocate their resources more efficiently. For instance, candidates in the signal subset may have priority for more focused study, while those in the noise subset can be removed; and, for

candidates in the indistinguishable subset, additional data may be collected to further separate weak signals from the noise (Conneely and Boehnke (2010), Spencer et al. (2009), Suresh and Chandrashekhara (2012), etc.).

The proposed framework of three-subset categorization helps to enrich current studies in multiple testing, which largely focus on the dichotomy of rejecting versus not rejecting null hypotheses. By controlling false positives, multiple testing procedures identify strong signals with high confidence. Popular criteria for false positive control include family-wise error (FWER) control (Dudoit et al. (2003), Dudoit et al. (2004), etc.) and false discovery rate (FDR) control (Benjamini and Hochberg (1995, 2000)). Recent developments in multiple testing focus on improving the power of FDR procedures and controlling FDR under dependence (Genovese and Wasserman (2004), Storey et al. (2004), Abramovich et al. (2006), Sun and Cai (2007), Efron (2007), Fan et al. (2012), etc.). These studies, however, would not provide informative results for the weak signals that are indistinguishable from the noise as these signals cannot be separated by controlling the selection of the noise alone. The higher the dimensionality is, the more indistinguishable signals are, and the less efficient the criterion of false positive control could be. This limitation can hinder meaningful applications of multiple testing procedures in ultra-high dimensional data analysis.

To delineate the indistinguishable and noise subsets would require an adaptive bound for the range of the weak signals. As the signals are often very sparse compared to the amount of noise, it is a challenging task to provide a statistical framework to characterize the weak signals. For instance, power analysis in multiple testing is well known to be difficult due to the limited information about the true signals. Another example is in variable selection, where screening procedures are developed to identify and then remove the noise subset (Fan and Lv (2008), Hall and Miller (2009), Fan et al. (2009), Fan et al. (2011), Zhu et al. (2011), Li et al. (2012), etc.). While significant efficiency has been demonstrated for these methods in handling ultra-high dimensional data, setting a good screening parameter remains a difficult problem as

it depends on the proportion and intensity of the non-zero coefficients, which are hard to be inferred from the data. Because of the inherent difficulty of weak signal inference, even though the phenomenon of three subsets has been frequently observed (e.g. Drton and Perlman (2008)), no rigorous statistical studies have been developed to explore the properties of the three subsets, neither is an efficient categorization method available up-to-date.

In this paper, we demonstrate the existence of the signal, noise, and indistinguishable subsets in Section 2 and connect the results with some recent developments in exact signal recovery. An efficient data-driven procedure called Two-Level Thresholding (TLT) is proposed in Section 3 to identify the three subsets by estimating the separation points d_* and d_{**} . d_* is estimated by the first level threshold \hat{d}_* , which strongly controls false positives and only selects strong signals with high probability. The more challenging part is the construction of \hat{d}_{**} , the second level threshold for the separation point between the indistinguishable and noise subsets. We develop a data-driven step-down procedure that traverses the ordered p -values until all signals are likely to be included. We show that, under certain conditions, only signals are included in the identified signal subset while the remaining signals are included in the identified indistinguishable subset with high probability.

Besides controlling false positives and false negatives, the proposed TLT procedure adapts to the intensity of the signal, so that the two thresholding levels move closer to each other as signals become stronger and the indistinguishable subset reduces in size. In the case when all signals are strong enough to be well-separated from the noise, the two thresholding levels converge to a single point.

The construction of TLT is completely data-driven. No prior information of the data distribution is needed; neither are tuning parameters involved in the algorithm. The computation is very fast with complexity $O(n \log n)$. These properties meet the needs of high-dimensional data applications.

The rest of the paper is organized as follows. We first demonstrates the existence

of the three subsets in section 2. Then we introduce the construction of the TLT procedure with its theoretical properties for the identification of the three subsets in Section 3. Monte Carlo simulations are presented in Section 4 to compare the results of TLT with those of the methods based on FDR control. Real-data results are provided in Section 5 where we apply our procedure to analyze SNP array data. We conclude in Section 6 with further discussions. The proofs are relegated to the Appendix.

2 Existence of The Three Subsets

In this section we first present the sufficient and almost necessary conditions for the existence of the signal, noise, and indistinguishable subsets. The results are connected to the recent developments in exact signal recovery. A simulation example is shown to demonstrate the relationship between the sizes of the three subsets and the signal intensity. To allow a succinct theoretical study, we assume, in this section, that the observations are generated independently from a normal mixture, i.e.,

$$X_i \sim N(0, 1)1_{\{i \in S_0\}} + N(\mu, 1)1_{\{i \in S_1\}}, \quad i \in \{1, \dots, n\}. \quad (2)$$

The following theorem shows the sufficient and almost necessary conditions for the existence of the three subsets.

Theorem 2.1 *Assume model (2). Then, asymptotically, the sufficient and almost necessary condition for the existence of the signal subset is*

$$\mu \geq \sqrt{2(1 + \epsilon) \log |S_0|} - \sqrt{2 \log |S_1|}, \quad (3)$$

for the existence of the indistinguishable subset is

$$\mu \leq \sqrt{2(1 - \epsilon) \log |S_0|} + \sqrt{2 \log |S_1|}, \quad (4)$$

and for the existence of the noise subset is

$$\log |S_1| \leq (1 - \epsilon) \log |S_0|, \quad (5)$$

for any $\epsilon > 0$.

Theorem 2.1 implies that (a) all three subsets exist when signals are sparse ($|S_1| = o(n)$) and the signal intensity is between the two bounds in (3) and (4); (b) when signal intensity is too small ($\mu < \sqrt{2(1+\epsilon)\log|S_0|} - \sqrt{2\log|S_1|}$), no signals stand outside the range of the noise, and only the indistinguishable and noise subsets exist; and (c) when signal intensity is large enough ($\mu > \sqrt{2(1-\epsilon)\log|S_0|} + \sqrt{2\log|S_1|}$), all signals are excluded from the range of the noise, and only the signal and noise subsets exist. Moreover, (4) shows that the higher the dimensionality is, the more likely that the indistinguishable subset exists.

2.1 Connection to Exact Signal Recovery

It is interesting to note that the sufficient and almost necessary condition for the existence of the indistinguishable subset is closely related to the condition for exact signal recovery in Ji and Jin (2012) and in Xie et al. (2011). Adopting the similar calibrations:

$$\pi = |S_1|/n = n^{-\beta}, \quad 0 < \beta < 1, \quad \text{and} \quad \mu = \mu_n = \sqrt{2r \log n}, \quad r > 0, \quad (6)$$

we have the following result.

Corollary 2.1 *Assume model (2) with calibration (6). Then, asymptotically, the noise subset always exists, and the sufficient and almost necessary condition for the existence of the signal subset is*

$$r > (1 - \sqrt{1 - \beta})^2, \quad (7)$$

and for the indistinguishable subset is

$$r < (1 + \sqrt{1 - \beta})^2. \quad (8)$$

Note that condition (8) delineates the complementary set of the exact recovery region in Ji and Jin (2012). In other words, only when the indistinguishable subset does not

exist is it possible to recover all signals with probability ≈ 1 . It is also interesting to see that condition (7) coincides with the detection boundary for the maximum statistic $M_n = \max_{1 \leq i \leq n} \{X_i\}$ (Donoho and Jin 2004). This shows that only when the signal subset exists is it possible for the maximum statistic M_n to separate the hypotheses $H_0 : X_i \sim N(0, 1), 1 \leq i \leq n$ and $H_a : X_i \sim N(0, 1)1_{\{i \in S_0\}} + N(\mu, 1)1_{\{i \in S_1\}}, 1 \leq i \leq n$.

2.2 A Simulation Example

The simulation example in this section demonstrates the relationship between the signal intensity and the sizes of the three subsets. The performance of the proposed TLT procedure is also presented in this example. We generated 10,000 observations and calculate their p -values, among which 2% are from $N(\mu, 1)$ and the rest from $N(0, 1)$. We set μ at 3, 4, and 7.5. When $\mu = 3$, $(d_*, d_{**}) = (65, 3090)$; when $\mu = 4$, $(d_*, d_{**}) = (116, 928)$; and when $\mu = 7.5$, $(d_*, d_{**}) = (200, 200)$. The three subsets and (d_*, d_{**}) are delineated in Figure 1 (a) in log-scale for better view. It is clear that, as μ increases, the signal subset increases to include all true signals, and the indistinguishable subset decreases to an empty set.

For the above example with $\mu = 4$ and $(d_*, d_{**}) = (116, 928)$, the distribution of the ranks of the signals is presented in Figure 1 (b). Our estimates $(\hat{d}_*, \hat{d}_{**}) = (72, 357)$, and clearly $\hat{d}_* < d_*$, so that $p_{(1)}, \dots, p_{(\hat{d}_*)}$ are all from signals. $\hat{d}_{**} = 357$, however, is much smaller than $d_{**} = 928$, but $p_{(1)}, \dots, p_{(\hat{d}_{**})}$ include 197 out of 200 signals, suggesting it as a reasonable estimate for the separation between the indistinguishable and noise regions. For comparison, the cut-off point of the FDR procedure in Benjamini and Hochberg (1995) (BH-FDR) with the control level conventionally set at 0.05 is 172, which means BH-FDR selects $p_{(1)}, \dots, p_{(172)}$ from the ordered p -values. The cut-off point of BH-FDR is between \hat{d}_* and \hat{d}_{**} , and larger than d_* . Apparently, BH-FDR selects more signals than \hat{d}_* and a few noise, but still missing many of the signals.

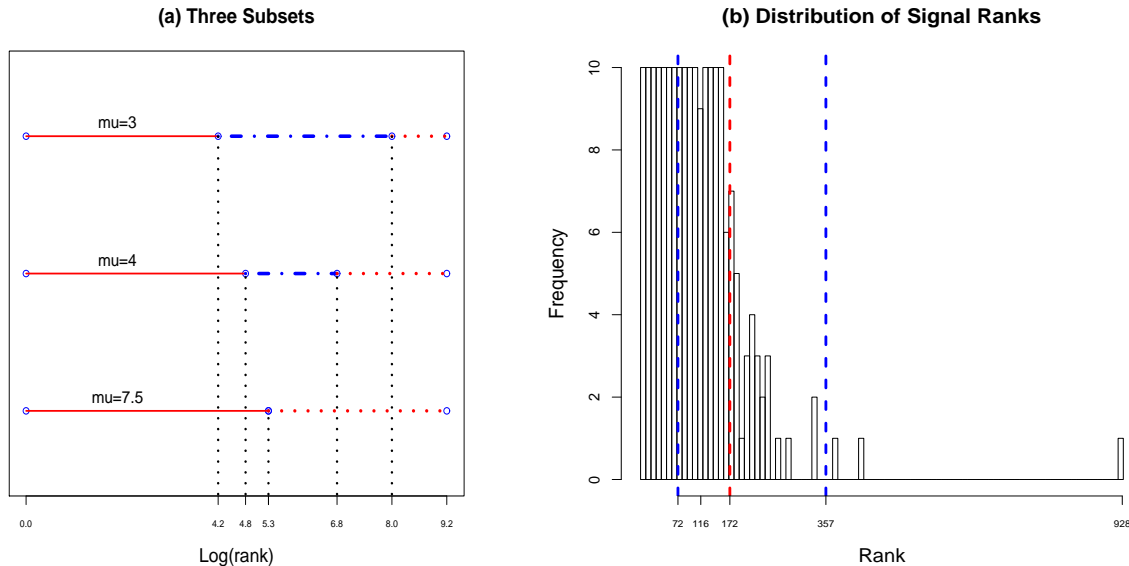


Figure 1: (a) Three subsets on the rank sequence of ordered p -values in log-scale. Signal subset (solid line), indistinguishable subset (dash-and-dot line), and noise subset (dot line) are separated by d_* and d_{**} . (b) Distribution of the signal ranks when $\mu = 4$. (d_* , d_{**}) are indicated at (116, 928). Vertical lines at 72 and 357 represents the locations of (\hat{d}_* , \hat{d}_{**}). The vertical line at 172 represents the location of the BH-FDR threshold.

3 Identification of The Three Subsets

In this section, we first construct the TLT procedure to estimate the separation points between the signal and indistinguishable subsets and between the indistinguishable and noise subsets, respectively. Similar to other adaptive procedures in multiple testing, we start with an estimate of the signal proportion $\pi = |S_1|/(|S_0 \cup S_1|)$. Various estimators have been developed in the literature under certain conditions on the data distribution. For example, Genovese and Wasserman (2004) and Meinshausen and Rice (2006) proposed two proportion estimators under a “purity” condition on the signal p -values. Cai et al. (2007), Jin and Cai (2007), and Jin (2008) developed proportion estimators for normally distributed observations. Given an esti-

mate $\hat{\pi}$ for the signal proportion, our estimator for the separation between the signal and indistinguishable subsets is defined as

$$\hat{d}_* = \max\{i : p_{(i)} < \frac{\alpha_n}{(1 - \hat{\pi})n}\}, \quad (9)$$

where α_n is the tolerance level for false positives and $\alpha_n \rightarrow 0$ as $n \rightarrow \infty$. The choice of the convergence speed of α_n depends on how stringently one wants to control the family-wise type I error. Reasonable choice can be $\alpha_n = 1/\log n$. \hat{d}_* can be regarded as an adaptive Bonferonni threshold. Its property of controlling false positives is relatively straightforward. The more challenging part is the construction of \hat{d}_{**} , the estimate of the separation between the indistinguishable and noise subsets. Even with the help of an estimate for signal proportion, one still does not know where the separation is since the signals are mixed with noise in the indistinguishable subset. Simply cutting at $\hat{\pi}n$ can include a lot of noise and miss many signals. We propose a data-driven procedure that traverses the ordered p -values until all signals are likely to be included. This cut is defined as

$$\hat{d}_{**} = \begin{cases} \hat{d}_*, & \hat{\pi}n \leq \hat{d}_*, \\ \hat{\pi}n + \min\{j \geq 1 : p_{(\hat{\pi}n+j)} \leq F_{(j)}^{-1}(\beta_n)\}, & \text{otherwise,} \end{cases} \quad (10)$$

where $F_{(j)}^{-1}$ is the inverse cumulative distribution function of $\text{Beta}(j, (1 - \hat{\pi})n - j + 1)$, β_n is the tolerance level for false negatives, and $\beta_n \rightarrow 0$ as $n \rightarrow \infty$. A reasonable choice can be $\beta_n = 1/\log n$. It is easy to see that \hat{d}_{**} is always greater than or equal to \hat{d}_* . In the case when $\hat{\pi}n \leq \hat{d}_*$, all signals are likely to rank before \hat{d}_* , then there is no need to go further along the ordered p -values, and we set $\hat{d}_{**} = \hat{d}_*$. On the other hand, $\hat{\pi}n > \hat{d}_*$ means that some signals are missing in the first \hat{d}_* ordered p -values, so that we need to go further to find all the signals. The search for \hat{d}_{**} starts at $\hat{\pi}n$, which is the estimated number of signals, and ends at the smallest j where $p_{(\hat{\pi}n+j)}$ is no greater than the β_n -quantile of $\text{Beta}(j, (1 - \hat{\pi})n - j + 1)$, which is the distribution of the j -th ordered p -value from $(1 - \hat{\pi})n$ noise. The intuition here is that, suppose that not all signals rank before \hat{d}_{**} , then the number of noise in $p_{(1)}, \dots, p_{(\hat{d}_{**})}$ is likely

to be greater than $\hat{d}_{**} - \hat{\pi}n$. Denote $\hat{j} = \hat{d}_{**} - \hat{\pi}n$, then the \hat{j} -th ordered p -value from $(1 - \hat{\pi})n$ noise is smaller than $p_{(\hat{d}_{**})}$. This event, however, has a small probability β_n due to the construction of \hat{d}_{**} where $p_{(\hat{d}_{**})} \leq F_{(j)}^{-1}(\beta_n)$.

Next, we present theoretical results on the properties of the two thresholding levels \hat{d}_* and \hat{d}_{**} . For simplicity, we utilize the proportion estimator of Meinshausen and Rice (2006), which is also constructed based on p -values. The estimator, defined as

$$\hat{\pi} = \max_{1 < i < n/2} \frac{i/n - p_{(i)} - \sqrt{2 \log \log n/n} \sqrt{p_{(i)}(1 - p_{(i)})}}{1 - p_{(i)}}, \quad (11)$$

is plugged into (9) and (10). Other proportion estimators can be used in the constructions of \hat{d}_* and \hat{d}_{**} in a similar way. The $\hat{\pi}$ in (11) is a consistent estimator under the following conditions as presented in Theorem 2 and 3 in Meinshausen and Rice (2006). Let $\pi = n^{-C}$ for some $C \in [0, 1)$. Assume either

$$C \in [0, 1/2) \quad \text{and} \quad \inf_{t \in (0,1)} G'(t) = 0, \quad (12)$$

or

$$C \in [1/2, 1) \quad \text{and} \quad \text{for all } q \in (0, 1), \quad \lim_{n \rightarrow \infty} (\log G^{-1}(q)) / (\log n) = -r, \quad r > 2(C - 1/2). \quad (13)$$

Condition (12) considers relatively dense signals with $\pi n \gg \sqrt{n}$; and all we need is the ‘‘purity’’ condition $\inf_{t \in (0,1)} G'(t) = 0$ (Genovese and Wasserman (2004), Meinshausen and Rice (2006)). Condition (13) considers sparse signals with $\pi n \leq \sqrt{n}$. In this case, stronger condition is needed for signal intensity, which is implied by (13).

Now we show that with high probability, only signals are ranked before \hat{d}_* and the number of signals ranked before \hat{d}_{**} converges to $|S_1|$, the total number of signals.

Let

$$n_0(d) = \text{number of noise in } \{p_{(1)}, \dots, p_{(d)}\} \quad \text{and} \quad n_1(d) = \text{number of signals in } \{p_{(1)}, \dots, p_{(d)}\}$$

for any integer $d \geq 1$.

Theorem 3.1 *Assume model (1) and condition (12) or (13). Then with high probability, only signals are ranked before the 1st thresholding level \hat{d}_* , and the number of signals ranked before the 2nd thresholding level \hat{d}_{**} converges to the total number of signals. That is, as $n \rightarrow \infty$,*

$$P(n_0(\hat{d}_*) > 0) \rightarrow 0 \quad (14)$$

and

$$P\left(\frac{n_1(\hat{d}_{**})}{|S_1|} < 1 - \epsilon\right) \rightarrow 0 \quad (15)$$

for any $\epsilon > 0$.

Theorem 3.1 shows that \hat{d}_* and \hat{d}_{**} are conservative estimates, which control false positives and false negatives respectively. While one can always achieve conservative estimates at 0 and n , the proposed estimators move closer to each other as signals become stronger and the indistinguishable subset gets smaller. When all signals are strong enough to be well-separated from the noise, \hat{d}_* and \hat{d}_{**} converge to a single point. This adaptivity property of the TLT procedure is presented in the following theorem with $\bar{G} = 1 - G$ defined as the survival function of G .

Theorem 3.2 *Assume model (1). If signals are strong enough, such that $\pi n \bar{G}(n^{-r}) \rightarrow 0$ for some $r > 1$. Then, with high probability, the indistinguishable subset does not exist, and for any α_n satisfying $\log n \ll \log \alpha_n \ll 0$, the signal and noise subsets are consistently separated by $\hat{d}_* = \hat{d}_{**}$. That is,*

$$P(\hat{d}_* = \hat{d}_{**} = |S_1|) \rightarrow 1 \quad (16)$$

as $n \rightarrow \infty$.

An intuitive understanding for the condition $\pi n \bar{G}(n^{-r}) \rightarrow 0$, $r > 1$, is that $\bar{G}(n^{-r}) \ll 1/\pi n = 1/n^{1-C} = o(1)$, which means that the total mass of G is asymptotically between 0 and n^{-r} . Note that the expectation of the smallest p -value from n noise is n^{-1} . Therefore, with $r > 1$, all the p -values of signals are well-separated from all the p -values of noise.

Theorem 3.1 and 3.2 are developed for \hat{d}_* and \hat{d}_{**} with $\hat{\pi}$ defined as in (11). If other proportion estimators are used, conditions in the theorems will be changed accordingly. For example, the proportion estimator in Cai et al. (2007) is designed for normally distributed noise and signals. Utilizing the additional properties of the distribution, this estimator is consistent under a weaker condition on the signal intensity in the sparse scenario compared to (13) (Cai et al. 2007). The theoretical properties of \hat{d}_* and \hat{d}_{**} in identifying the signal, noise, and indistinguishable subsets can be proved in a similar way.

In real applications, data may not satisfy the conditions for the existence of a consistent proportion estimator. However, prior knowledge can often allow practitioners to provide a possible range for the signal proportion. We demonstrate that the study of signal, noise, and indistinguishable subsets can still be carried out utilizing such prior knowledge. Suppose π is bounded by

$$\pi^- \leq \pi \leq \pi^+. \quad (17)$$

Define

$$\tilde{d}_* = \max\{i : p_{(i)} < \frac{\alpha_n}{(1 - \pi^-)n}\}, \quad (18)$$

and

$$\tilde{d}_{**} = \begin{cases} \tilde{d}_*, & \pi^+ n \leq \tilde{d}_*, \\ \pi^+ n + \min\{j \geq 1 : p_{(\pi^+ n + j)} \leq \tilde{F}_{(j)}^{-1}(\beta_n)\}, & \text{otherwise,} \end{cases} \quad (19)$$

where $\tilde{F}_{(j)}^{-1}$ is the inverse cumulative distribution function for Beta($j, (1 - \pi^-)n - j + 1$). The next theorem states that the modified version \tilde{d}_* and \tilde{d}_{**} can still serve as conservative estimates for the separation points d_* and d_{**} .

Theorem 3.3 *Assume model (1) and condition (17). Then, with high probability, only signals are ranked before \tilde{d}_* , and the number of signals ranked before \tilde{d}_{**} converges to the total number of signals. That is, as $n \rightarrow \infty$,*

$$P(n_0(\tilde{d}_*) > 0) \rightarrow 0 \quad (20)$$

and

$$P(n_1(\tilde{d}_{**}) < |S_1|) \rightarrow 0. \quad (21)$$

Although $(\tilde{d}_*, \tilde{d}_{**})$ may not be as close as $(\hat{d}_*, \hat{d}_{**})$ gets to (d_*, d_{**}) , they can provide useful information of the signal, noise, and indistinguishable subsets in many applications where conditions for the consistency of proportion estimation are hard to be satisfied and some informative prior knowledge of the signal proportion is available.

4 Simulation

In this section, we demonstrate, via simulation studies, the finite sample performance of the TLT procedure on the identification of the signal, noise, and indistinguishable subsets. In each example, 10,000 observations are generated, in which the noise data points are sampled from $N(0, \sigma)$ and signals from $N(\mu, 1)$. The selections of \hat{d}_* and \hat{d}_{**} with $\alpha_n = \beta_n = 1/(2 \log n) \approx 0.05$ are compared with those of the BH-FDR with $\alpha = 0.05$ (Benjamini and Hochberg 1995) and the adaptive FDR (Benjamini and Hochberg (2000), Genovese and Wasserman (2004)). Setting α_n at $1/(2 \log n)$ for $n = 10,000$ results in a control level close to the conventional level (0.05) used by other methods, so that the results from different methods are comparable. β_n is set to be equal to α_n for simplicity.

Among the methods compared, BH-FDR is easiest to implement, while the others require estimating the signal proportion. The estimates \hat{d}_* and \hat{d}_{**} , the cut-off point of BH-FDR (t_{FDR}), the cut-off point of the adaptive FDR (t_{aFDR}), as well as the number of false positives (FP) and the number of false negatives (FN) for each procedure are computed. We repeatedly generate the observations and compute performance measures for 100 times in each simulation example. The median and mean absolute deviation (MAD) of these measures are reported for more robust comparison results against the outliers in the 100 replications.

Example 1 shows the effect of signal intensity. Set $\sigma = 1$ and $\pi = 0.01$. Signal

mean μ varies from 2.5 to 5.5. Since the signal proportion is very small, the results of BH-FDR and the adaptive FDR are very close. To save space, the results of the latter are omitted in this example. Figure 2 presents the histograms of \hat{d}_{**} from the 100 replications for $\mu = 2.5$ and 5.5. It shows that as signal intensity increases, the distribution of \hat{d}_{**} becomes more concentrated.

Table 1 shows that the cut-off point of BH-FDR (t_{FDR}) is between \hat{d}_* , the estimate of the separation between the signal and indistinguishable subsets (S-I Separation), and \hat{d}_{**} , the estimate of the separation between the indistinguishable and noise subsets (I-N Separation). As signal intensity increases, the indistinguishable subset shrinks and the cut-off locations of all three procedures move closer. As to the accuracy of identifying the signal, noise, and indistinguishable subsets, it is shown that the FPs of \hat{d}_* and t_{FDR} are well controlled with t_{FDR} having a bit higher FP when signal intensity increases. This agrees with our intuition since BH-FDR applies a less stringent rule to control false positives. FP of \hat{d}_{**} however is not controlled as it is not supposed to be. Interesting results are shown for the FN of \hat{d}_{**} . Among the 100 signals, the proportions of mis-specified signals of \hat{d}_{**} are 28%, 11%, 3%, and 1% for $\mu = 2.5, 3.5, 4.5, 5.5$, respectively. Compared with the FN of t_{FDR} , which has mis-specified proportions of 92%, 48%, 12%, and 1%, \hat{d}_{**} has many fewer false negatives when signals are only moderately strong. This simulation shows that the proposed estimators \hat{d}_* and \hat{d}_{**} adapt to the signal intensity, and the identified indistinguishable subset between \hat{d}_* and \hat{d}_{**} shrinks with increasing μ .

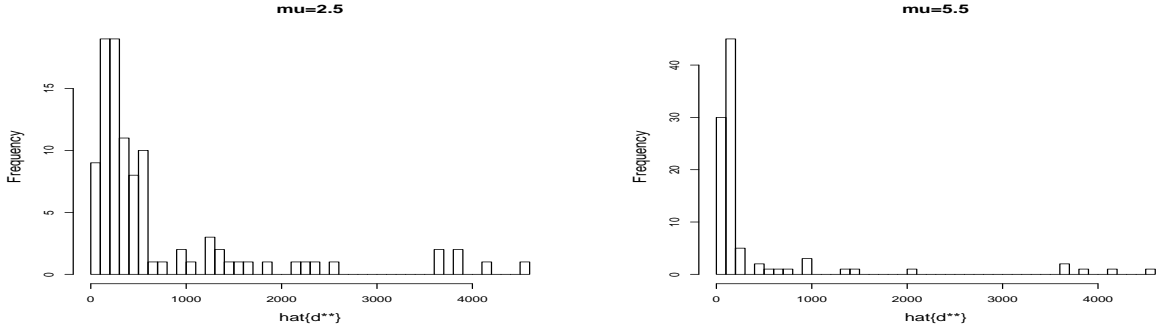


Figure 2: Histograms of \hat{d}_{**} for $\mu = 2.5$ and 5.5 from 100 replications.

Table 1: Effect of signal intensity. Median and MAD (in parentheses) of \hat{d}_* , t_{FDR} , \hat{d}_{**} , and their corresponding FP and FN over 100 replications. π is fixed at 1%.

	S-I Separation			BH-FDR			I-N Separation		
	\hat{d}_*	FP	FN	t_{FDR}	FP	FN	\hat{d}_{**}	FP	FN
$\mu = 2.5$	3(1)	0(0)	97(1)	8(4)	0(0)	92(4)	325(269)	261(253)	28(19)
$\mu = 3.5$	17(3)	0(0)	83(3)	54(7)	2(1)	48(6)	194(113)	103(97)	11(9)
$\mu = 4.5$	54(4)	0(0)	46(5)	92(4)	4(3)	12(3)	126(44)	29(34)	3(3)
$\mu = 5.5$	86(3)	0(0)	14(3)	103(1)	4(1)	1(1)	104(9)	4(3)	1(1)

Example 2 demonstrates the effect of signal proportion. Set $\sigma = 1$ and $\mu = 3$. The signal proportion π changes from 1% to 20%. As shown in Table 2, when π increases, FP of \hat{d}_* remains around 0. FN of \hat{d}_{**} is also fairly robust over the different numbers of signals. BH-FDR and adaptive FDR, on the other hand, increases in both FP and FN with increasing signal proportion.

Table 2: Effect of signal proportion. μ is fixed at 3.

$ S_1 $	S-I Separation			BH-FDR			adapFDR			I-N Separation		
	\hat{d}_*	FP	FN	t_{FDR}	FP	FN	t_{aFDR}	FP	FN	\hat{d}_{**}	FP	FN
100	8(3)	0(0)	92(3)	27(7)	1(1)	74(6)	27(7)	1(1)	74(6)	227(140)	147(135)	21(12)
500	40(6)	0(0)	460(6)	255(14)	11(4)	255(13)	259(13)	12(4)	253(13)	1119(494)	645(462)	31(28)
1000	81(8.9)	0(0)	919(9)	637(21)	28(4)	392(18)	647(18)	31(4)	386(18)	1960(589)	996(548)	38(31)
2000	172(11)	0(0)	1828(10)	1485(29)	59(9)	575(28)	1543(32)	72(11)	529(24)	3224(660)	1268(614)	46(32)

Example 3 has heterogenous noise generated for 10% of the observations. With

signal intensity and proportion fixed at $\mu = 3.5$ and $\pi = 1\%$, the proportion of heterogeneous noise is 10 times the proportion of signals. This example demonstrates a common scenario in real-data applications where unjustified artifacts causes heterogeneity in the background noise. The heterogeneous noise in this example are randomly generated from $N(0, \sigma)$ with $\sigma \sim \text{Gamma}(2, \theta)$. Let the scale parameter θ vary from 0.5 to 2, which results in increasing variability for the noise. Due to the small signal proportion, the results of the adaptive FDR are very close to those of the BH-FDR and omitted in this example. Table 3 shows that FPs of all procedures increase with θ . FNs, on the other hand, are very stable. Theorem 3.3 provides some explanation for the robustness of \hat{d}_{**} in controlling false negatives. Since heterogeneous noise can result in large jumps, the estimated proportion $\hat{\pi}$ is larger than the true π . Constructed using this $\hat{\pi}$, \hat{d}_{**} is essentially the \tilde{d}_{**} in (19), which is built on an upper bound of the true π . The theoretical property on false negative control is presented in (21).

Table 3: *Robustness for heterogeneous noise. Set $\mu = 3.6$ and $\pi = 1\%$.*

	S-I Separation			BH-FDR			I-N Separation		
	\hat{d}_*	FP	FN	t_{FDR}	FP	FN	\hat{d}_{**}	FP	FN
$\theta = 0.5$	22(4)	5(3)	82(3)	69(9)	15(4)	45(6)	196(67)	107(60)	12(7)
$\theta = 1$	53(7)	35(6)	81(4)	132(12)	71(9)	38(4)	443(180)	347(174)	7(4)
$\theta = 1.5$	94(10)	75(9)	80(4)	195(15)	130(13)	35(4)	556(230)	459(223)	7(3)
$\theta = 2$	134(12)	113(10)	80(4)	249(12)	182(10)	33(4)	556(179)	466(175)	9(4)

Example 4 generates autocorrelated observations with $\rho_{ij} = a^{|i-j|}$ for $a = 0, 0.5, 0.7$ and 0.9. The number of observations are reduced to 1,000 to save computation time. Set $\sigma = 1$, $\pi = 0.05$, $\mu = 3$, and $\alpha_n = \beta_n = 1/\log n$. The results summarized in Table 4 are quite stable over different values of the autocorrelation parameter a with \hat{d}_{**} having slightly better control on false negatives for large a .

Table 4: *Robustness under autocorrelation. Set $\pi = 0.05$ and $\mu = 3$.*

	S-I Separation			BH-FDR			I-N Separation		
	\hat{d}_*	FP	FN	t_{FDR}	FP	FN	\hat{d}_{**}	FP	FN
$a = 0$	14(3)	0(0)	36(3)	27(4)	1(1)	25(4)	74(45)	30(33)	7(7)
$a = 0.5$	13(4)	0(0)	37(4)	24(7)	1(1)	27(7)	69(35)	27(28)	7(7)
$a = 0.7$	13(7)	0(0)	37(6)	28(9)	1(1)	24(7)	67(44)	25(33)	5(8)
$a = 0.9$	14(13)	0(0)	36(13)	29(17)	0(0)	20(15)	72(51)	27(41)	3(4)

5 Real Application

We apply the three-subset identification to the genotyping data from the Autism Genetics Resource Exchange (AGRE) collection (Bucan et al. 2009) generated by high-throughput single nucleotide polymorphism (SNP) array technology. Genotypes in this data set are measured in Log R ratio (LRR), which is calculated at each SNP location as $\log_2(R_{obs}/R_{exp})$, where R_{obs} is the observed total intensity of both major and minor alleles and R_{exp} is computed from a reference genome (Peiffer et al. 2006). LRR data are widely used for detecting copy number variants (CNVs), in which the goal is to identify genomic regions with deletion or duplication of DNA segments (Feuk et al. 2006). Such DNA mutations have been reported to play important roles in population diversity and disease association (McCarroll and Altshuler 2007). Due to the fact that the intensity ratio deviates from the baseline in CNV segments, various segment detection methods have been developed to detect CNVs based on SNP array data (Olshen et al. (2004), Zhang et al. (2010), Siegmund et al. (2010), Jeng et al. (2010), Jeng et al. (2012), etc.)

In this paper, instead of just providing a list of candidates for CNVs, we provide more insight of the data by identifying the signal, noise, and indistinguishable subsets. We specifically consider the observations on Chromosome 19 for three individuals, which are collected from 9501 SNPs for each individual. The signals are copy number deletions, which may cause LRR to be negative. For a given individual,

LRR observations are first normalized, and then the likelihood ratio is calculated for each interval with length $\leq L$ as in Jeng et al. (2010). The likelihood ratio of an interval is defined as the standardized sum of observations in that interval, and L is set at 20 as most of the CNVs cover less than 20 SNPs (Zhang et al. 2009). There are $n = 9501 \times 20 = 190,020$ such likelihood ratio statistics for each individual. When the distribution of LRR changes in an interval, the corresponding likelihood ratio is expected to deviate from the baseline. Figure 3 demonstrates the distribution of the likelihood ratios for all the intervals with length $\leq L$ on Chromosome 19 of one individual. The outliers in the left tail are likely to come from copy number deletions. The plots are similar for other individuals and are, thus, omitted.

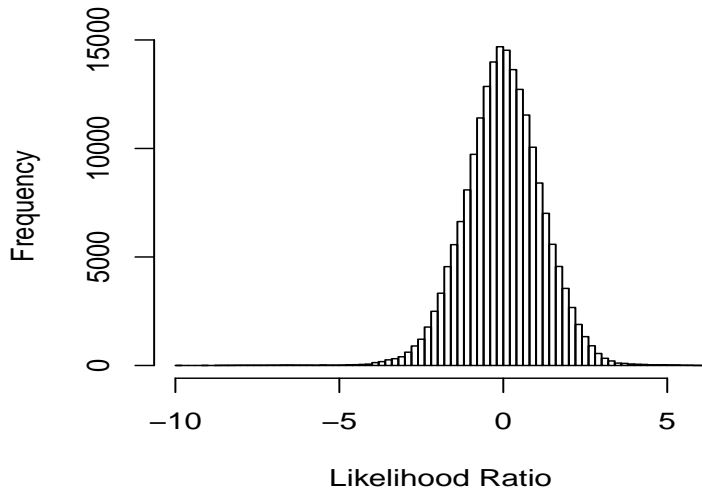


Figure 3: *Histogram of the likelihood ratios of the intervals on Chromosome 19.*

We calculate the p -values for these likelihood ratios assuming that the background noise follow $N(0, 1)$ after normalization. The likelihood ratios are locally dependent due to the fact that the intervals are short and overlapping. In this example we treat them as independent observations to illustrate the method. The separations among signal, indistinguishable, and noise subsets are determined by either \hat{d}_* (9) and \hat{d}_{**} (10) or \tilde{d}_* (18) and \tilde{d}_{**} (19). We find that estimating the signal proportion by (11)

seems to result in a much larger proportion estimate than commonly expected for SNP array data, possibly due to the artifacts involved in the data generation process (Marioni et al. 2007). Thus, we use a more reasonable bound of $0 \leq \pi \leq 0.005$ for this data set. Setting the upper bound at 0.005 means that the copy number deletions on Chromosome 19 are approximately less than 50 (Zhang et al. 2009). The signal, noise, and indistinguishable subsets are identified by deriving the cut-off points \tilde{d}_* and \tilde{d}_{**} . Because the intervals are overlapping, we only keep intervals having minimum p -values among overlapping segments to indicate the locations of copy number deletions. All the other intervals overlapping with them are removed. \tilde{d}_* and \tilde{d}_{**} are then re-defined as the ranks among these non-overlapping intervals. For the three individuals, $(\tilde{d}_*, \tilde{d}_{**})$ are (2, 18), (1, 76), and (1, 36), respectively.

We further perform validation on the identified signal, noise, and indistinguishable subsets. The candidates in each subset are compared to the reported members in a CNV database maintained in The Centre for Applied Genomics (<http://projects.tcag.ca/variation/project.html>). A candidate region can overlap with zero, one, or more than one CNVs in the database. The mean value of the number of such CNVs in the database is presented for each subset in Table 5. In other words, let O_j = number of CNVs in the database that overlap with the j -th candidate in the list of ranked intervals. Define $\text{ovlap-s} = \text{mean}(O_j, 1 \leq j \leq \tilde{d}_*)$, $\text{ovlap-i} = \text{mean}(O_j, \tilde{d}_* < j \leq \tilde{d}_{**})$, $\text{ovlap-n} = \text{mean}(O_j, \tilde{d}_{**} < j \leq \text{total number of intervals})$. Table 5 shows that these mean values, in general, decrease from ovlap-s to ovlap-n . For example, in the identified indistinguishable subset of individual 3, 6.8 CNVs in the database overlap with each candidate in the identified indistinguishable subset on average, while the number decreases to 2.0 for the identified noise subset. This agrees with our intuition for the three subsets as larger mean values represents stronger evidence for identifying the true CNVs. One exception is ovlap-s for individual 3. There is only one candidate in the identified signal subset, which happens to be missed in the database. A possible explanation is that this candidate is a de novo CNV only car-

ried by individual 3. The sample correlation between the interval length and O_j are 0.17, 0.28, and 0.26 for the three individuals, respectively, indicating that the trend observed in Table 5 is not likely caused by the length factor.

Table 5: *Estimated separations, \tilde{d}_* and \tilde{d}_{**} , and the mean value of O_j in each subset.*

	ovlap-s	\tilde{d}_*	ovlap-i	\tilde{d}_{**}	ovlap-n
Individual 1	10.5	2	3.4	18	2.5
Individual 2	4	1	4.7	76	2.1
Individual 3	0	1	6.8	36	2.0

6 Further Discussion

In this paper, we developed a novel statistical framework and an efficient TLT procedure to categorize the data into the signal, noise, and indistinguishable subsets. This unique categorization can provide further insight for the data and help the practitioners to design more appropriate follow-up studies to identify the true signals in different subsets. Another motivation for the new development is its potential to provide an objective criterion for sample-size determination based on the cardinality of the indistinguishable subset. Unlike traditional sample-size calculation, which is based on a pre-specified level of signal intensity, we may determine whether the sample size is large enough by examining the size of the indistinguishable subset.

Additional insight for the quality of the data may also be achieved by examining the indistinguishable subset. For example, a large indistinguishable subset suggests that there are many small non-null observations, which are either true signals or, very often, caused by artifacts involved during the data generation. Investigating the sources of possible artifacts in follow-up studies may significantly reduce the indistinguishable subset and result in better separation between signals and noise.

We developed two related TLT schemes, one is completely data-driven, the other

utilizes prior knowledge on the possible range of the signal proportion. Such flexibility allows practitioners to meet the needs of various applications. The computation for both procedures are very fast.

The study in this paper is based on p -values. Other statistics carrying information about signal intensity, such as the local FDR values (Efron (2007), Sun and Cai (2007)) may be used in place of p -values. It will be interesting to investigate this possibility in future research.

In this paper, we assumed independent p -values to allow a succinct theoretical study of the new method. Simulation examples in section 4 demonstrate the robustness of the proposed method for autocorrelated observations. We plan to study in depth the three-subset categorization under dependence in future works. We find the recent paper by Fan et al. (2012) to be very helpful. According to their work, it is possible to estimate the arbitrary dependence structure of the p -values and transform the dependent p -values into weakly dependent ones.

Last but not least, estimating the separation point between the indistinguishable and noise subsets can be related to the problem of variable screening in high-dimensional regression and can provide new insights on the well-known challenge of screening parameter selection in high-dimensional data analysis.

Acknowledgement

We thank Dr. Leonard Stefanski and Dr. John Daye for helpful discussions and comments.

Appendix: Proofs

The proofs for theorems in section 2 and 3 are provided. A preliminary lemma is first introduced to summarize part of the results in Theorem 1 and 2 in Meinshausen and

Rice (2006). The proof of the lemma is omitted.

Lemma 6.1 *Assume the same conditions as in Theorem 3.1. Let $\hat{\pi}$ be defined as in (11). Then for any given $\epsilon > 0$,*

$$P((1 - \epsilon)\pi \leq \hat{\pi} \leq \pi) \rightarrow 1$$

as $n \rightarrow \infty$.

Proof of Theorem 2.1

It is sufficient to show the following claims. For any $\epsilon > 0$,

$$P(\nexists \text{ signal subset}) = o(1) \quad \text{given} \quad \mu \geq \sqrt{2(1 + \epsilon) \log |S_0|} - \sqrt{2 \log |S_1|}, \quad (22)$$

$$P(\exists \text{ signal subset}) = o(1) \quad \text{given} \quad \mu \leq \sqrt{2(1 - \epsilon) \log |S_0|} - \sqrt{2 \log |S_1|}, \quad (23)$$

$$P(\nexists \text{ indist. subset}) = o(1) \quad \text{given} \quad \mu \leq \sqrt{2(1 - \epsilon) \log |S_0|} + \sqrt{2 \log |S_1|}, \quad (24)$$

$$P(\exists \text{ indist. subset}) = o(1) \quad \text{given} \quad \mu \geq \sqrt{2(1 + \epsilon) \log |S_0|} + \sqrt{2 \log |S_1|}. \quad (25)$$

$$P(\nexists \text{ noise subset}) = o(1) \quad \text{given} \quad \log |S_1| \leq (1 - \epsilon) \log |S_0|, \quad (26)$$

$$P(\exists \text{ noise subset}) = o(1) \quad \text{given} \quad \log |S_1| \geq (1 + \epsilon) \log |S_0|. \quad (27)$$

Consider (22) first.

$$\begin{aligned} P(\nexists \text{ signal subset}) &= P(\max\{X_i, i \in S_1\} \leq \max\{X_i, i \in S_0\}) \\ &\leq P(\max\{X_i, i \in S_1\} \leq \sqrt{2 \log |S_0|}) + P(\max\{X_i, i \in S_0\} > \sqrt{2 \log |S_0|}) \\ &\leq P(\max\{X_i, i \in S_1\} \leq \sqrt{2 \log |S_0|}) + o(1), \end{aligned} \quad (28)$$

where the last inequality is by the extreme value theory of standard normal random variables. Also,

$$\begin{aligned} &P(\max\{X_i, i \in S_1\} \leq \sqrt{2 \log |S_0|}) \\ &= P(\max\{X_i, i \in S_1\} - \mu \leq \sqrt{2 \log |S_0|} - \mu) \\ &= P(\max\{X_i, i \in S_1\} - \mu \leq \sqrt{2 \log |S_1|} + (\sqrt{2 \log |S_0|} - \mu - \sqrt{2 \log |S_1|})) \\ &\leq P(\max\{X_i, i \in S_1\} - \mu \leq \sqrt{2 \log |S_1|} + (\sqrt{2 \log |S_0|} - \sqrt{2(1 + \epsilon) \log |S_0|})) \\ &= o(1), \end{aligned} \quad (29)$$

where the inequality is by $\mu > \sqrt{2(1+\epsilon)\log|S_0|} - \sqrt{2\log|S_1|}$. Combining (28) and (29) gives (22).

Next consider (23).

$$\begin{aligned}
& P(\exists \text{ signal subset}) \\
&= P(\max\{X_i, i \in S_1\} > \max\{X_i, i \in S_0\}) \\
&\leq P(\max\{X_i, i \in S_1\} > \sqrt{2\log|S_0|} - \log\log n) + P(\max\{X_i, i \in S_0\} < \sqrt{2\log|S_0|} - \log\log n) \\
&\leq P(\max\{X_i, i \in S_1\} > \sqrt{2\log|S_0|} - \log\log n) + o(1), \tag{30}
\end{aligned}$$

where the last inequality is by the extreme value theory of standard normal random variables. Also,

$$\begin{aligned}
& P(\max\{X_i, i \in S_1\} > \sqrt{2\log|S_0|} - \log\log n) \\
&= P(\max\{X_i, i \in S_1\} - \mu > \sqrt{2\log|S_1|} + (\sqrt{2\log|S_0|} - \log\log n - \mu - \sqrt{2\log|S_1|})) \\
&\leq P(\max\{X_i, i \in S_1\} - \mu > \sqrt{2\log|S_1|} + (\sqrt{2\log|S_0|} - \log\log n - \sqrt{2(1-\epsilon)\log|S_0|})) \\
&= o(1), \tag{31}
\end{aligned}$$

where the inequality is by $\mu \leq \sqrt{2(1-\epsilon)\log|S_0|} - \sqrt{2\log|S_1|}$. Combining (30) and (31) gives (23).

The claims in (24) - (27) can be proved in similar ways.

□

Proof of Theorem 3.1

Consider (14) first. Since

$$\begin{aligned}
P(n_0(\hat{d}_*) > 0) &\leq P(\exists i \in S_0 : P_i \leq \frac{\alpha_n}{(1-\hat{\pi})n}) \\
&\leq (1-\pi)n \cdot P(P_i \leq \frac{\alpha_n}{(1-\pi)n}, \hat{\pi} \leq \pi) + P(\hat{\pi} > \pi) \\
&\leq \alpha_n + o(1),
\end{aligned}$$

where the third inequality is by Lemma 6.1 and the fact that p -values from noise are uniformly distributed. Then (14) follows.

Next, consider (15). Define $n_1 = |S_1|$. Recall that $\hat{j} = \hat{d}_{**} - \hat{\pi}n$, then

$$\begin{aligned}
P(n_1(\hat{d}_{**}) \leq (1 - \epsilon)n_1) &= P(n_0(\hat{d}_{**}) > \hat{d}_{**} - (1 - \epsilon)n_1) \\
&= P(n_0(\hat{d}_{**}) > \hat{\pi}n + \hat{j} - (1 - \epsilon)\pi n) \\
&= P(n_0(\hat{d}_{**}) > (\hat{\pi} - (1 - \epsilon)\pi)n + \hat{j}) \\
&\leq P(n_0(\hat{d}_{**}) > (\hat{\pi} - (1 - \epsilon)\pi)n + \hat{j}, \hat{\pi} \geq (1 - \epsilon)\pi) + P(\hat{\pi} < (1 - \epsilon)\pi) \\
&\leq P(n_0(\hat{d}_{**}) > \hat{j}) + o(1), \tag{32}
\end{aligned}$$

where the first equality is by $\hat{d}_{**} = n_0(\hat{d}_{**}) + n_1(\hat{d}_{**})$, the second equality is by $n_1 = \pi n$, and the last step is by Lemma 6.1.

In the case of $\hat{\pi}n \leq \hat{d}_*$, we have $\hat{d}_{**} = \hat{d}_* = \hat{\pi}n$ and $\hat{j} = 0$. Then

$$P(n_0(\hat{d}_{**}) > \hat{j}) = P(n_0(\hat{d}_*) > 0) \rightarrow 0 \tag{33}$$

by (14). (15) follows by combining (32) and (33).

In the case of $\hat{\pi}n > \hat{d}_*$, define $P_{(j)}^0$ as the j -th smallest p -value from n_0 noise. Then

$$\begin{aligned}
P(n_0(\hat{d}_{**}) > \hat{j}) &\leq P(P_{(j)}^0 < p_{(\hat{d}_{**})}) \\
&\leq P\left(\text{Beta}(\hat{j}, n_0 - \hat{j} + 1) < F_{(j)}^{-1}(\beta_n)\right) \\
&\leq P\left(\text{Beta}(\hat{j}, (1 - \hat{\pi})n - \hat{j} + 1) < F_{(j)}^{-1}(\beta_n), \hat{\pi} \leq \pi\right) + P(\hat{\pi} > \pi) \\
&= \beta_n + o(1), \tag{34}
\end{aligned}$$

where the first inequality is because when the elements from S_0 are more than \hat{j} in $\{1, \dots, \hat{d}_{**}\}$, the \hat{j} th smallest p -value from S_0 must rank before the p -value at \hat{d}_{**} . The second inequality is by the well-known fact that $P_{(j)}^0 \sim \text{Beta}(j, n_0 - j + 1)$ and the construction of \hat{d}_{**} , where $p_{(\hat{d}_{**})} \leq F_{(j)}^{-1}(\beta_n)$. The last step is by the definition of $F_{(j)}^{-1}$ and Lemma 6.1. Combining (32) and (34) gives (15).

Proof of Theorem 3.2

Defines events $A = \{\hat{d}_* \geq \hat{\pi}n\}$, $B = \{\hat{d}_* \leq \pi n\}$, and $C = \{\hat{\pi}n = \pi n\}$. By the construction of \hat{d}_* in (9), it is enough to show that

$$P(A \cap B \cap C) \rightarrow 1,$$

which is implied by

$$P(A^c) + P(B^c) + P(C^c) \rightarrow 0. \quad (35)$$

Consider $P(A^c)$ first.

$$\begin{aligned} P(A^c) &\leq P(\hat{d}_* < \pi n) + P(\hat{\pi} > \pi) \\ &\leq P(\exists i \in S_1 : P_i > \frac{\alpha_n}{(1-\hat{\pi})n}) + o(1) \\ &\leq \pi n \bar{G}(\frac{\alpha_n}{(1-\hat{\pi})n}) + o(1) \\ &\leq \pi n \bar{G}(n^{-r}) + o(1) = o(1), \end{aligned}$$

where the second inequality is by the construction of \hat{d}_* in (9) and Lemma 6.1, the fourth inequality is by $\frac{\alpha_n}{(1-\hat{\pi})n} > n^{-r}$ when $\alpha_n \gg n^{-c}$ and $r > 1$, and the last step is by the condition $\pi n \bar{G}(n^{-r}) \rightarrow 0$.

For $P(B^c)$, it is easy to show that $P(B^c) = P(n_0(\hat{d}_*) > 0) \rightarrow 0$ by similar arguments leading to (14).

Now consider $P(C^c)$. By lemma 6.1, it is enough to show that

$$P(\hat{\pi}n \leq \pi n - 1) \rightarrow 0,$$

which is implied by

$$P(\frac{\hat{\pi}}{\pi} - 1 < -\frac{1}{\pi n}) \rightarrow 0. \quad (36)$$

Define

$$F_n(t) = \frac{1}{n} \sum_{i=1}^n 1(P_i \leq t), \quad U_{n_0}(t) = \frac{1}{n_0} \sum_{i=1}^{n_0} 1(P_i^{(0)} \leq t), \quad G_{n_1}(t) = \frac{1}{n_1} \sum_{i=1}^{n_1} 1(P_i^{(1)} \leq t).$$

Then, by the construction of $\hat{\pi}$ in (11), for any $t \in [0, 1]$,

$$\begin{aligned} \frac{\hat{\pi}}{\pi} - 1 &\geq \frac{F_n(t) - t - \pi}{\pi} - \frac{\sqrt{2 \log \log n} \sqrt{t(1-t)}}{\pi \sqrt{n}} \\ &= \frac{(1-\pi)U_{n_0}(t) + \pi G_{n_1}(t) - t - \pi}{\pi} - \frac{\sqrt{2 \log \log n} \sqrt{t(1-t)}}{\pi \sqrt{n}} \\ &= (G(t) - 1) + (G_{n_1}(t) - G(t)) + \frac{1-\pi}{\pi}(U_{n_0}(t) - t) - t - \frac{\sqrt{2 \log \log n} \sqrt{t(1-t)}}{\pi \sqrt{n}}. \end{aligned}$$

Let $t = n^{-r}$. Then by condition $\pi n \bar{G}(n^{-r}) \rightarrow 0$ and $r > 1$,

$$|G(t) - 1| = \bar{G}(n^{-r}) = o\left(\frac{1}{\pi n}\right),$$

$$|G_{n_1}(t) - G(t)| = O_p\left(\sqrt{\frac{G(t)(1 - G(t))}{n_1}}\right) = O_p\left(\sqrt{\frac{\bar{G}(n^{-r})}{\pi n}}\right) = o_p\left(\frac{1}{\pi n}\right),$$

$$\frac{1 - \pi}{\pi} |U_{n_0}(t) - t| = O_p\left(\frac{1 - \pi}{\pi} \sqrt{\frac{t(1 - t)}{n_0}}\right) = O_p\left(\frac{\sqrt{1 - \pi}}{\pi} \frac{1}{n^{(1+r)/2}}\right) = o_p\left(\frac{1}{\pi n}\right),$$

$$\frac{\sqrt{2 \log \log n} \sqrt{t(1 - t)}}{\pi \sqrt{n}} = \frac{\sqrt{2 \log \log n}}{\pi} \frac{1}{n^{(1+r)/2}} = o\left(\frac{1}{\pi n}\right).$$

Therefore, (36) follows. Combining the above results for $P(A^c)$, $P(B^c)$, and $P(C^c)$ gives (35).

Proof of Theorem 3.2

The proof of this theorem is similar to that of Theorem 3.1 and is, thus, omitted to save space.

References

- Abramovich, F., Benjamini, Y., Donoho, D., and Johnstone, I. (2006), “Adapting to Unknown Sparsity by Controlling the False Discovery Rate,” *Ann. Statist.*, 34, 584–653.
- Benjamini, Y. and Hochberg, Y. (1995), “Controlling the False Discovery Rate: a practical and powerful approach to multiple testing,” *J. Royal Stat. Soc. B*, 57, 289–300.
- (2000), “On the Adaptive Control of the False Discovery Rate in Multiple Testing with Independent Statistics,” *J. of Educational and Behavioral Statistics*, 25, 60–83.

- Bucan, M., Abrahams, B., Wang, K., Glessner, J., Herman, E., Sonnenblick, L., Retuerto, A. A., Imielinski, M., Hadley, D., Bradfield, J., Kim, C., Gidaya, N., Lindquist, I., Hutman, T., , Sigman, M., Kustanovich, V., Lajonchere, C., Singleton, A., Kim, J., , Wassink, T., McMahon, W., Owley, T., Sweeney, J., Coon, H., Nurnberger, J., Li, M., Cantor, R., Minshew, N., Sutcliffe, J., Cook, E., Dawson, G., Buxbaum, J., Grant, S., Schellenberg, G., Geschwind, D., and Hakonarson, H. (2009), “Structural variation in the human genome,” *PLoS Genetics*, 5.
- Cai, T., Jin, J., and Low, M. (2007), “Estimation and Confidence Sets For Sparse Normal Mixtures,” *Ann. Statist.*, 35, 2421–2449.
- Conneely, K. N. and Boehnke, M. (2010), “META-ANALYSIS OF GENETIC ASSOCIATION STUDIES AND ADJUSTMENT FOR MULTIPLE TESTING OF CORRELATED SNPS AND TRAITS,” *Genetic Epidemiology*, 34(7).
- Donoho, D. and Jin, J. (2004), “Higher criticism for detecting sparse heterogeneous mixtures,” *Ann. Statist.*, 32, 962–994.
- Drton, M. and Perlman, M. D. (2008), “A SINful approach to Gaussian graphical model selection,” *Journal of Statistical Planning and Inference*, 138(4).
- Dudoit, S., Shaffer, J. P., and Boldrick, J. C. (2003), “Multiple Hypothesis Testing in Microarray Experiments,” *Statist. Sci.*, 18(1), 71–103.
- Dudoit, S., van der Laan, M., and Pollard, K. S. (2004), “Multiple Testing. Part I. Single-Step Procedures for Control of General Type I Error Rates,” *Statistical Applications in Genetics and Molecular Biology.*, 3, article 13.
- Efron, B. (2007), “Size, Power AND False Discovery Rates,” *The Annals of Statistics*, 35, 1351–1377.
- Fan, J., Feng, Y., and Song, R. (2011), “Nonparametric independence screening in

- sparse ultra-high dimensional additive models,” *J. of American Statistical Association*, 116, 544–557.
- Fan, J., Han, X., and Gu, W. (2012), “Control of the false discovery rate under arbitrary covariance dependence,” *J. of American Statistical Association*, 107, 1019–1045.
- Fan, J. and Lv, J. (2008), “Sure Independence Screening for Ultra-High Dimensional Feature Space,” *J. R. Statist. Soc. B*, 70, 849–911.
- Fan, J., Samworth, R., and Wu, Y. (2009), “Ultra-Dimensional Variable Selection via Independent Learning: Beyond the Linear Model,” *J. of Machine Learning Research*, 10, 1829–1853.
- Feuk, L., Carson, A., and Scherer, S. (2006), “Structural variation in the human genome,” *Nature Review Genetics*, 7.
- Genovese, C. and Wasserman, L. (2004), “A stochastic process approach to false discovery control,” *Ann. Statist.*, 32, 1035–1061.
- Hall, P. and Miller, H. (2009), “Using Generalized Correlation to Effect Variable Selection in Very High Dimensional Problems,” *J. of Computational and Graphical Statistics*, 18, 533550.
- Jeng, X. J., Cai, T. T., and Li, H. (2010), “Optimal sparse segment identification with application in copy number variation analysis,” *J. Am. Statist. Ass.*, 105, 1156–1166.
- (2012), “Simultaneous Discovery of Rare and Common Segment Variants,” *Biometrika*, To appear.
- Ji, P. and Jin, J. (2012), “UPS delivers optimal phase diagram in high-dimensional variable selection,” *Ann. Statist.*, 40, 73–103.

- Jin, J. (2008), “Proportion of nonzero normal means: oracle equivalence and uniformly consistent estimators,” *J. of the Royal Statistical Society, Series B*, 70, 461–493.
- Jin, J. and Cai, T. (2007), “Estimating the null and the proportion of non-null effects in large-scale multiple comparisons,” *J. American Statistical Association*, 102, 495–506.
- Li, R., Zhong, W., and Zhu, L. (2012), “Feature screening via distance correlation learning,” *J. of American Statistical Association*, In press.
- Marioni, J. C., Thorne, N. P., Valsesia, A., Fitzgerald, T., Redon, R., Fiegler, H., Andrews, T. D., Stranger, B. E., Lynch, A. G., Dermitzakis, E. T., Carter, N. P., Tavar, S., and Hurles, M. E. (2007), “Breaking the waves: improved detection of copy number variation from microarray-based comparative genomic hybridization,” *Genome Biology*, 8(10).
- McCarroll, S. S. and Altshuler, D. M. (2007), “Copy-number variation and association studies of human disease,” *Nature Genetics*, 39.
- Meinshausen, M. and Rice, J. (2006), “Estimating the proportion of false null hypotheses among a large number of independent tested hypotheses,” *Ann. Statist.*, 34, 373–393.
- Olshen, A. B., Venkatraman, E. S., Lucito, R., and Wigler, M. (2004), “Circular binary segmentation for the analysis of array-based DNA copy number data,” *Biostatistics*, 5 (4).
- Peiffer, D. A., Le, J. M., Steemers, F. J., Chang, W., Jenniges, T., Garcia, F., Haden, K., Li, J., Shaw, C. A., Belmont, J., Cheung, S. W., Shen, R. M., Barker, D. L., and Gunderson, K. L. (2006), “High-resolution genomic profiling of chromosomal aberrations using Infinium whole-genome genotyping,” *Genome Res*, 16.

- Siegmund, D. O., Yakir, B., and Zhang, N. R. (2010), “Detecting simultaneous variant intervals in aligned sequences,” *Annals of Applied Statistics*, 5, 645–668.
- Spencer, C., Su, Z., Donnelly, P., and Marchini, J. (2009), “Designing genome-wide association studies: sample size, power, imputation, and the choice of genotyping chip,” *PLoS Genetics*, 5(5).
- Storey, J. D., Taylor, J. E., and Siegmund, D. (2004), “Strong control, conservative point estimation and simultaneous conservative consistency of false discovery rates: a unified approach,” *J. of the Royal Statistical Society: Series B*, 66, 187–205.
- Sun, W. and Cai, T. (2007), “Oracle and Adaptive Compound Decision Rules for False Discovery Rate Control,” *J. American Statistical Association*, 102, 901–912.
- Suresh, K. and Chandrashekhara, S. (2012), “Sample size estimation and power analysis for clinical research studies,” *Journal of Human Reproductive Sciences*, 5(1).
- Xie, J., Cai, T., and Li, H. (2011), “Sample size and power analysis for sparse signal recovery in genome-wide association studies,” *Biometrika*, 98, 273–290.
- Zhang, F., Gu, W., Hurles, M., and Lupski, J. (2009), “Copy number variation in human health, disease and evolutions,” *Annual Review of Genomics and Human Genetics*, 10, 451–481.
- Zhang, N. R., Siegmund, D. O., Ji, H., and Li, J. (2010), “Detecting Simultaneous Change-points in Multiple Sequences,” *Biometrika*, 97, 631–645.
- Zhu, L., Li, L., Li, R., and Zhu, L.-X. (2011), “Model-free feature screening for ultrahigh dimensional data,” *J. of American Statistical Association*, 106, 1464–1475.